The Programmable Permanent Magnet Actuator: A Paradigm Shift in Efficiency for Low-Speed Torque-Holding Robotic Applications

Jean-Baptiste Chossat, Alexis Maslyczyk, Jean-Simon Lavertu, and Vincent Duchaine

***Abstract*—In this paper we propose a new type of electromagnetic actuator called the "Programmable Permanent Magnet" (PPM) actuator. The PPM actuator is designed to tackle low-speed high-torque applications where classic electromagnetic actuators are highly inefficient.**

The PPM actuator is based on the application of pulsed current to magnetize a hard ferromagnetic stator that is made of individual SmCo (custom grade) magnets placed in a Halbach array configuration. The motor creates a spring-like torque function that generates up to 0.2 N.m. Unlike electromagnetic actuators, by design the PPM actuator does not draw current while exerting torque. Instead, the motor's power consumption depends on its rotational speed or torque variations.

The PPM actuator is, by consequence, most efficient where classical electromagnetic motors are most inefficient, and is a new alternative to actuators for robotic applications, which tend to operate in low-speed, high-torque conditions.

The prototyped PPM actuator measures 47 mm in diameter, with a height of 35 mm and weight of 200 g, and has been successfully integrated in a commercially available 2-finger gripper from Robotiq, Inc.

***Index Terms*—Foundations of Automation, Product Design, Development and Prototyping, Compliant Joint/Mechanism, Robot Safety, Grasping.**

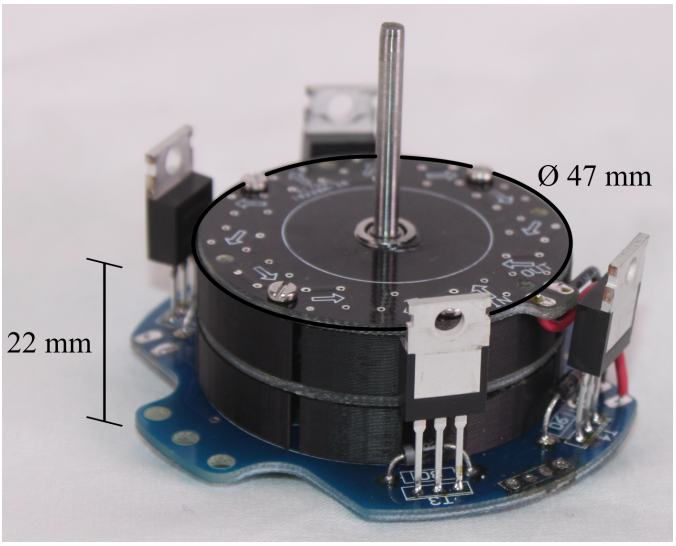

Figure 1: The PPM actuator.

I. Introduction

DESPITE great technological advancement, robots continue to lag behind human abilities to perform a variety of commonplace physical tasks. Even state-of-the-art robots like those seen at the Darpa Robotics Challenge are clumsy compared to humans. One reason for this is the present-day limits of robotic actuation.

Even though innovations in motors have brought about great improvements in, e.g., electric cars, they have not done the same for robots, because robots require a completely different type of actuation. It might seem surprising, but conventional electromagnetic motors are inherently ill-suited to robotic actuation.

Conventional motors, such as DC or brushless motors, reach high efficiency at high speeds (due to back electromotive force, or back EMF), but robotic applications typically require low-speed high-torque movements, for which conventional motors are much less efficient. This inefficiency has three consequences: *i.* robots consume so much power that they are unable to run on batteries for more than brief periods; *ii.* the amount of excess heat that is generated (as described by the Joule effect) results in damage to the motor; and *iii.* due to the risk of heat damage, the actuator's torque is limited.

The typical work-around to this problem has been to use gearboxes. By changing the ratio of speed to torque, gearboxes allow the motor to operate at a higher speed, which is more efficient. However, gearboxes introduce new issues such as backlash, additional weight, high reflected inertia during collisions, and sometimes non-backdriveability [14].

Another problem with gearboxes is that they do not help with efficiency in situations where a robot has to apply torque in a fixed position. This is particularly relevant to robots (as opposed to say, cars), because they frequently need to apply torque while not actually moving, such as while gripping an object or standing upright. Here, the motor at the robot's joint must maintain torque without rotating; and thus the motor is operating in the zero-efficiency zone (max. power input and zero power output).

Numerous attempts have been made to circumvent the shortcomings of conventional motors [15], [16], [9], [7], [17].

Manuscript received: September, 11, 2017; Revised November, 2, 2017; Accepted December, 24, 2017.

This paper was recommended for publication by Editor Han Ding upon evaluation of the Associate Editor and Reviewers' comments. This work was supported by the Natural Sciences and Engineering Research Council of Canada (NSERC) and Robotiq Inc.)

The authors are with the Control and Robotics laboratory, in the cole de Technologie Suprieure University, Montral, Qubec, Canada jbchossat@hotmail.com

Digital Object Identifier (DOI): see top of this page.

One method has been to improve the actuator's heat dissipation properties. Among the most successful examples is the water-cooled motor system that helped the SCHAFT team win the DARPA competition trials [15], [16]. Their robot's actuators were able to output higher torque because the excess heat was dissipated by a custom-built liquid cooling system. Although this is an ingenious method, it still does not address the root of the problem: the inefficiency of conventional motors in most robotic applications.

In light of these problems, we propose a fundamentally new approach to robotic actuation: the "Programmable Permanent Magnet" (PPM) actuator, which is illustrated in Fig. 1). The PPM actuator is capable of sustaining a variety of torques indefinitely, and for a given torque, the actuator's energy consumption is directly proportional to its velocity. To the best of our knowledge, this is the first actuator to have these characteristics, which are particularly promising for robotics applications.

Section II explains important concepts needed to understand the motor's operation. Section III presents the design of the prototype. Section V describes the experiments conducted with the prototype, and gives their results. Section VI concludes.

II. A Novel Paradigm for Torque Generation

A typical motor, such as a Maxon brushless motor, takes the electrical power that's supplied (P_{in}), and transforms it with some loss (P_{loss}) into mechanical power (P_{mech}), where the latter is a direct function of torque and rotational speed, thus allowing us to also calculate the efficiency (η). These relations are given by:

$$\begin{aligned} P_{in} &= P_{loss} + P_{mech}, \\ \eta &= \frac{P_{mech}}{P_{in}}, \end{aligned} \tag{1}$$

where

$$\begin{aligned} P_{in} &= Vi, \\ P_{mech} &= \tau\omega, \\ P_{loss} &= i^2 R, \end{aligned} \tag{2}$$

and where i is the actuator's current, V is its voltage, and R is the electrical resistance of the winding.

When a conventional motor operates at its maximum speed, it is not able to exert any torque. This point is known as no load speed, and when it is reached there is very little power output. However, the motor operates quite efficiently because it is not drawing much electrical power either, due to back EMF. This phenomenon balances the voltage applied across the windings, thereby reducing the effective current flow and heat generation in the windings.

As can be seen from Fig. 2 made using the datasheet of the Maxon brushless motor 339286, at slightly lower speeds (than max.), the motor exerts torque. Here it operates in a very efficient zone because it is converting almost all the electrical power into mechanical power. So at medium-to-high speed and torque, the motor is highly efficient.

However, at very low speeds the motor is also producing very little power, but this time there is not as much back EMF

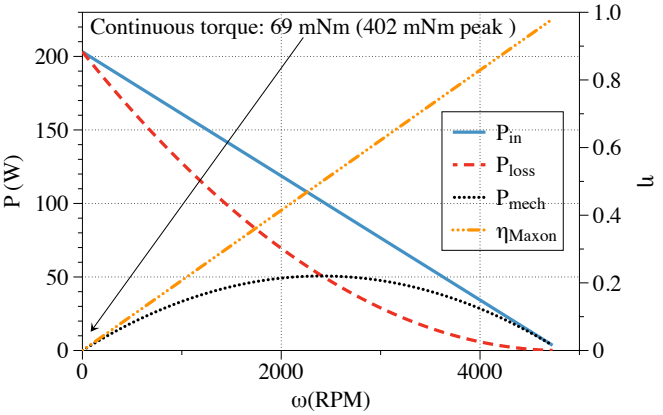

Figure 2: Maxon 339286 brushless motor power characteristics

to help lower the power input. Instead, the motor is consuming its maximum amount of electrical energy and when there is no speed, all of this energy is wasted in the form of heat. To summarize, conventional motors exhibit very good efficiency at high speeds, and very low efficiency at low speeds.

In both a DC motor and in our actuator, movement and torque are created by the interaction between two magnetic fields: one fixed (a permanent magnet), and one variable. However, whereas in a DC motor the variable field is a temporary electromagnetic field controlled by an electrical current, in our actuator, both the fixed and variable components are permanent magnets. We "set" the magnetic field of one permanent magnet to a given value, and create motion by constantly "resetting" this field.

To do so, our PPM actuator relies on current pulses to generate strong magnetic fields that will magnetize the hard ferromagnetic material of the windings. Hard and soft ferromagnetic materials are distinguished by their ability to retain magnetic fields: hard ferromagnetic materials are much more difficult to demagnetize than soft ferromagnetic materials.

In other words, in the PPM actuator, the current is used to magnetize magnets in the windings. The PPM actuator then generates torque due to the interaction between the magnetic fields of the stator and rotor. Assuming the magnets are neither heated past their Curie temperature nor physically battered, and that the hard ferromagnetic material can sustain the opposing magnetic field, then the "set" torque will be maintained by the actuator at no additional cost. The actuator only requires power to switch its magnets, in order to rotate its shaft, which happens when a pulse of current is sent through the windings. Therefore, as shown in Fig. 3, the PPM actuator's power input (P_{in}) is directly related to the number of these pulses (N_p) required to cause a single rotation, to the energy contained in each pulse (E_p), and to the actuator's angular velocity (ω). So we can approximate the PPM actuator's consumption with the following equation:

$$P_{in} = \frac{\omega}{2\pi} N_p E_p. \tag{3}$$

We can conclude from this equation that the power consumed by this new actuator is directly proportional to how

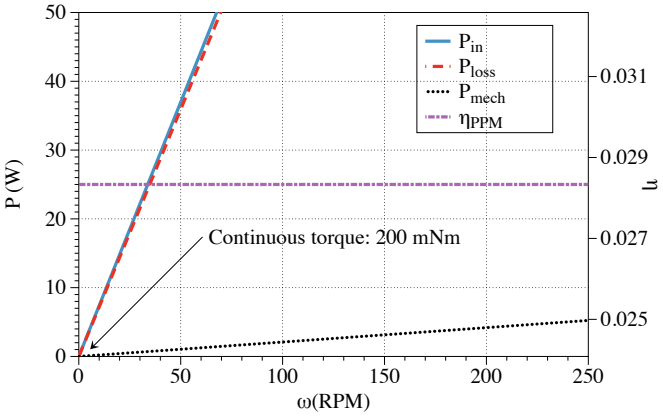

Figure 3: PPM actuator power characteristics.

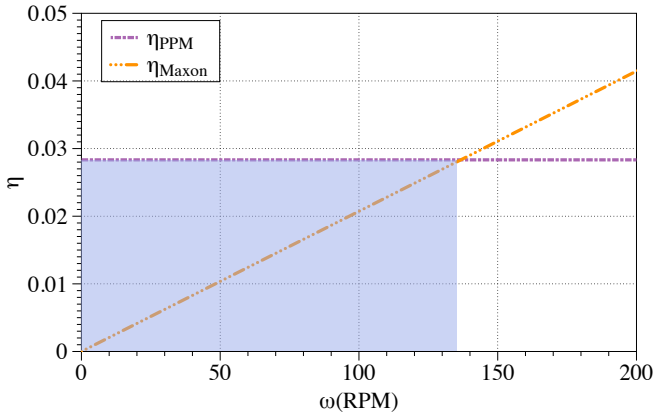

Figure 4: Low speed actuators efficiency comparison.

quickly it rotates. The only other variable in this equation is the energy contained in each pulse E_p, since the number of pulses is fixed during the actuator design (in our case, N_p = 4). The amount of energy used in these pulses controls the strength of the generated magnetic fields, which results in distinct levels of torque. To summarize, by adjusting those two variables (ω and E_p), we control both the velocity and the torque produced by the actuator.

This equation also suggests that the power consumption of the PPM actuator follows a trend that is the inverse of what a conventional motor would follow. Indeed, as can be seen from Fig.2, a DC brushless motor consumes less power as speed increases (due to back EMF), whereas our actuator's power consumption increases linearly as a function of speed. This line crosses the origin at zero, because the actuator is able to hold a given torque indefinitely without consuming any power. This linear relationship between power input and velocity also implies a very particular efficiency profile. Indeed as we can see from Eq. (4), the efficiency η of the PPM actuator for a given torque is a constant.

$$\eta_{PPM} = \frac{P_{mech}}{P_{in}} = \frac{\tau\omega}{\omega\frac{1}{2\pi}N_pE_p} = \frac{2\pi\tau}{N_pE_p} \tag{4}$$

Given that our actuator's efficiency is constant, it will inevitably intersect with the efficiency curve of a conventional motor (which starts with zero efficiency at zero speed). Illustrating this phenomenon, Fig.4 compares the efficiency of our PPM prototype with a Maxon 339286 DC brushless motor, of very similar diameter and length. The velocity associated with the point at which the two curves intersect represents the superior limit of the range of operations where our motor is always more efficient than a traditional motor. However, since efficiency is an instantaneous measurement, it may not be the best indicator of each actuator's merits for a given application. A more realistic indicator might be overall energy consumption. For example, applications like robotic grasping involve a great deal of torque-holding time. In tasks like these, the PPM actuator might consume less energy during the entire task than a conventional motor, even if it is (when rotating) occasionally less efficient than a conventional motor. The extent to which PPM actuator's efficiency is superior to a conventional motor is arguably quite limited. However, as mentioned above, our actuator is designed for low speed, high torque applications. Regarding this latter characteristic, we must point out that our actuator is able to sustain indefinitely a torque of 200 mNm when a comparable Maxon motor can only continuously produce 69mNm.

Another consequence of this particular power consumption profile is that, unlike conventional actuators wherein heat becomes an issue when the motor needs to hold a given torque steady, our actuator will start overheating as speed increases, since increasing the speed requires sending more pulses of energy per unit of time.

III. The PPM Actuator Design

A. Recent Approaches

One way to deal with the high torque demands of robots has been through static balancing, which has been promoted for increased robot compliance and human safety as well as reduced motor power consumption [4]. Different systems such as springs [13] or counter weight [10] have been proposed to achieve it.

Another recently proposed approach is to use the electromagnetic force contained in magnets to generate passive and active torque. For example, Knaian et al. created a variation of the stepper motor, the "Electropermanent" (EPM) actuator, that uses magnets to maintain friction between the stator and rotor [3], [8]. The same team also used this technology to create programmable matter [5] and electropermanent valves in a soft robot [12]. Their electropermanent actuator relies on a pair of magnets, with one made from a softer ferromagnetic material than the other. Together they form a magnetic circuit that can be switched through the softer magnet (AlNiCo) to form either a closed circuit with almost no magnetic flux escaping, or an open circuit where the magnetic flux is projected outside of the arrangement of magnets [3]. This same idea was modified for use in a drone latching mechanism, the "OpenGrab EPM" [2], where it enabled high payload while maintaining low power cost.

One of the limitations of using EPM in an actuator is that the arrangement of the two magnets produces a near-binary

function. Indeed, the external field can practically only be turned on and off. Moreover, due to the very high coercivity of the neodymium (NdFeB) magnet, it is impossible to reverse the direction of the external magnetic field.

Our approach instead uses only one type of magnet, for which the magnetization is changed via a pulse of current in a solenoid. This enables us to "set" any amount of magnetization, in any direction, within the physical limits of the magnet's magnetization. One of the challenges with this approach is finding the right magnet. AlNiCo magnets, for instance, are easy to magnetize and require little energy to control, but they are also easily demagnetized (low coercivity) and can only weakly retain magnetic fields (low effective remanence). This produces a weak actuator, since a strong internal core will easily demagnetize the AlNiCo magnet(s). On the other hand, some permanent magnets like NdFeB are not easily demagnetized by a strong permanent magnetic core, so they could enable a very strong actuator. However, the amount of energy required to program such a magnet is very high, making NdFeB a poor solution from the point of view of efficiency, and also one that would be difficult to implement. Thus, finding the right magnet requires finding the right trade-off between the magnet's strength and the magnetization cost.

B. Magnet Selection

The maximum product of a magnet's coercivity and remanence (BH_{max}) is frequently used to select magnets. However, since we want a magnet that is as powerful as possible while being easy to reprogram, the BH_{max} is not a good indicator of the ideal magnet for our actuator. The BH_{max} is an approximate value of the theoretical maximum energy stored in the magnet, whereas our magnets ideally require a combination of high remanence (B_r) and low intrinsic coercivity (H_{ci}). The intrinsic coercivity (H_{ci}) corresponds to the strength of the magnetizing field (H) to which a magnet must be subjected in order to completely lose its magnetization (M). The H_{ci} is a good measure of the energetic cost of magnetization of a given magnet. Although magnet coercivity (H_c) is more commonly used than H_{ci}, it only corresponds to the magnetization field required to *momentarily* cancel a magnet's magnetic field, as opposed to the field required to permanently demagnetize it, which in some cases is far greater. Fig. 5 shows the difference between the two types of coercivity and serves to remind the reader of magnets' hysteresis curves.

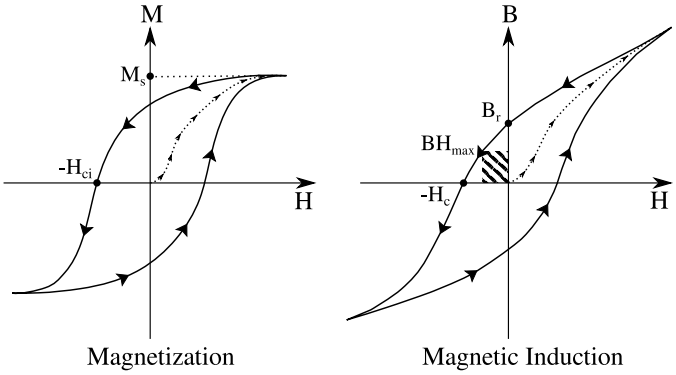

Figure 5: Typical ferromagnetic material hysteresis curves; independent scales.

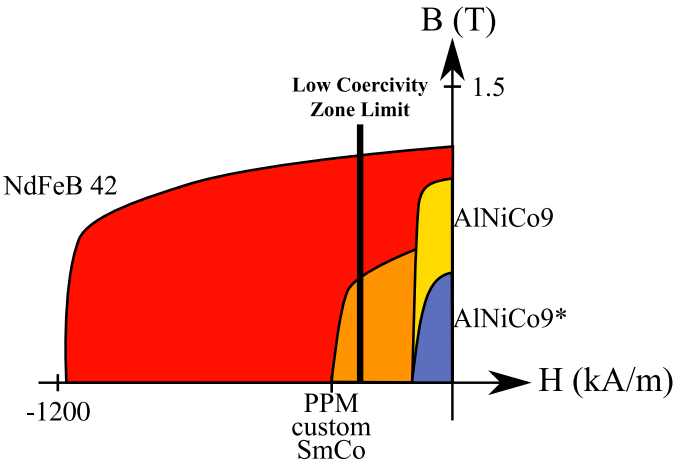

Figure 6: Second quadrant of the BH curve for the NbFeb42, YX-12 SmCo, and AlNiCo theoretical and *effective ferromagnetic materials [1].

Using these criteria may lead one to consider AlNiCo magnets. However, as explained before, their intrinsic coercivity is so weak that they cannot oppose a magnetic field without suffering demagnetization. Taking this into consideration, the criteria for selecting our magnet can be represented by the following function:

$$\begin{aligned} &\max\ f(x) = \frac{B_r}{H_{ci}} \\ &\text{subject to } H_{ci} \geq c, \end{aligned} \tag{5}$$

where B_r is expressed in mT, and H_{ci} in kA/m, and where c is the minimum intrinsic coercivity required to avoid demagnetization by the core of the actuator. Based on this, we commissioned custom-made SmCo-grade magnets that maximizes Eq. 5. Fig. 7 shows how our custom magnets perform for this function compared to other types of magnets. The intrinsic coercivity of our magnets (395 kA/m) is among the lowest of the SmCo magnet family, but is still several times the intrinsic coercivity of any AlNiCo magnet while also producing a magnetic flux density of 0.723 Tesla.

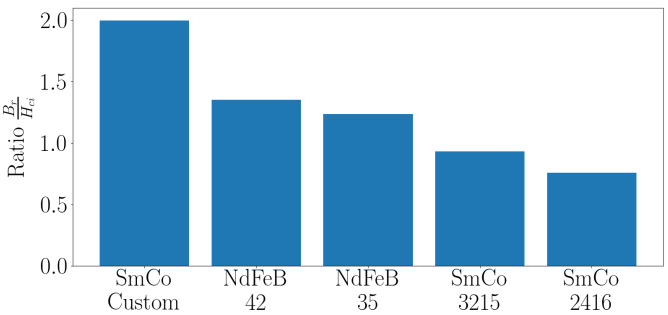

Figure 7: Comparison of different ferromagnetic materials [1] using the ratio proposed in Eq. 5.

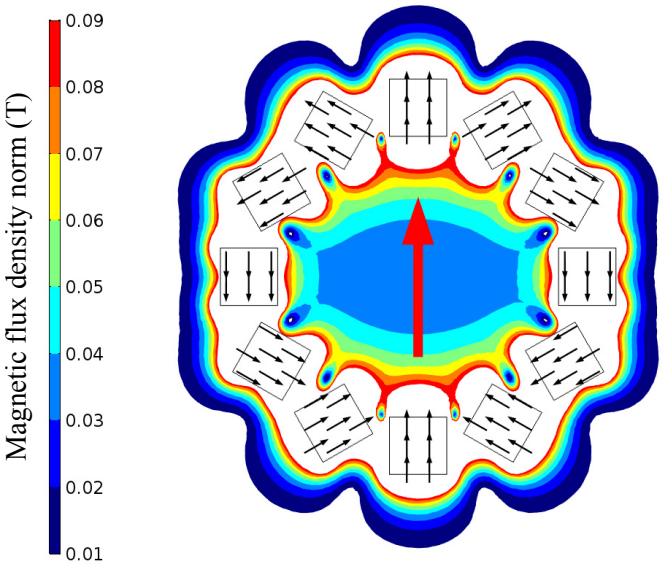

Figure 8: FEA magnetostatic simulation of the magnetic flux density norm (T) in one of our Halbach arrays.

As seen above, the PPM actuator is very inefficient at high speeds. Therefore, we may want to avoid using it with a transmission gear box. If a transmission is necessary, one with a very low ratio might be preferable. To avoid the need for a transmission, we need an actuator with a very high torque-to-volume ratio, which necessitates creating a strong magnetic field within the actuator.

C. Halbach Magnetic Circuit

To create this strong magnetic field, we used a special magnet arrangement called an Halbach array [11], [6]. As illustrated in Fig. 8, Halbach arrays have the remarkable characteristic of focusing the magnetic flux of individual magnets to create one stronger magnetic field on only one side of the structure. By focusing all the field in the center of the actuator, the Halbach array minimizes loss of the magnetic field outside the actuator, which also comes with the benefit of minimizing noise that may be induced in nearby devices like sensors. The number and direction of magnetic poles within the Halbach array depends on the magnets' configuration. In our case, we decided to use an Halbach array ($K = 1$) that creates a unique magnetic pole pair with near-uniform flux within the center of the stator [6].

As Boisclair et al. demonstrated [4], a passive Halbach array in configuration $K = 1$ produces a torque function that follows a sinusoid, which can be used to statically balance a single degree of freedom like a pendulum. Many dynamic systems follow a near-sinusoid function, such as the torque about the elbow joint of an industrial manipulator. We used a similar configuration ($K = 1$) in our actuator to benefit from how this near-sinusoid torque function matches some robotic applications. Specifically, the benefit is that the resulting actuator requires less energy because its torque can be adjusted less frequently, and less drastically, than would be the case if the torque function did not match the application at all.

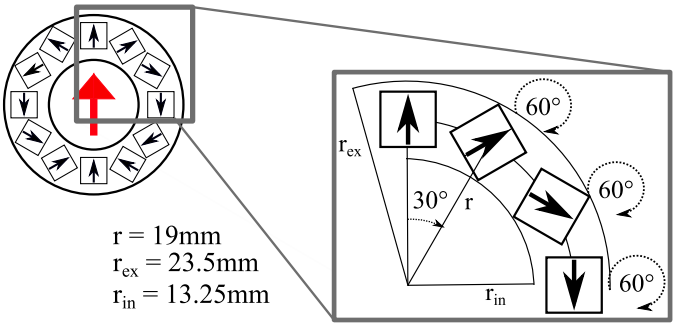

Figure 9: Halbach array magnet positioning.

The PPM is equipped with two Halbach arrays that are superposed one on top of the other, with a shifted angle of 90 degrees between them. This bipolar configuration allows us to produce the required torque (within the actuator's range) in any orientation, and to have the actuator rotate in any direction.

IV. Actuator Prototype

The actuator has two main components – stator and rotor – each of which is composed of two "stages" of permanent magnets. In order to maximize the strength of the generated magnetic field, we want to maximize the amount of magnetic material for a given volume of the PPM actuator. Consequently, we want to minimize the distance between each magnet – both within the Halbach arrays, and between the magnets of the arrays and the rotor.

Given that the Halbach array configuration dictates that the magnets have a certain orientation (see Fig. 9), in order to maximize the amount of magnet per unit of volume, we had to use relatively short magnets. The custom-made magnets used in the Halbach arrays are cylinders of 6.35 mm (0.25") in diameter and height, which are magnetized through the length. The stator is composed of two of these Halbach arrays, which are superposed and separated by 4.25 mm.

The rotor in our actuator is comprised of two hollow cylindrical magnets that are made of high-grade ferromagnetic material (N42 NdFeB) and are magnetized diametrically. These two magnets are also superposed and separated by 4.25 mm. Each magnet has the following dimensions: 25.4 mm (1") in diameter, with a hollow center of 3.175 mm (0.125") in diameter, and height of 6.35 mm (0.25").

It has been shown that using discrete magnets rather than a single magnet of continuously changing magnetization creates a weaker magnetic field, and more magnetic flux leakage. In the context of actuators, consequently, the amplitude of the torque function is reduced.

Therefore, we knew our results would be worse than what is predicted for an ideal Halbach array. To find out precisely how much worse, we simulated the magnetic flux density norm for all the permanent magnets within the actuator using a finite element analysis (FEA) software (Comsol Multiphysics). These simulations allowed us to evaluate both the strength of the magnetic field within the Halbach array, and the amount of magnetic flux that leaked outside of it.

Finally, we computed the PPM actuator's theoretical maximum axial torque while the rotor makes a full revolution.

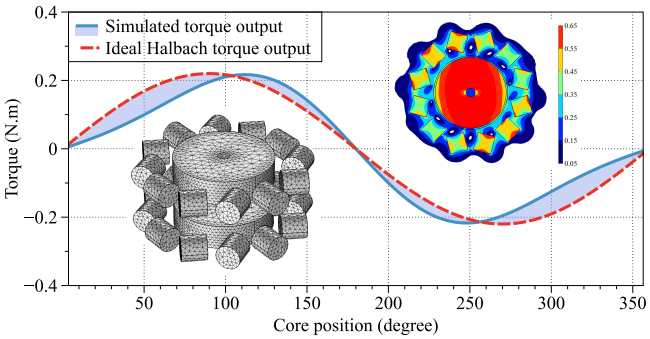

Figure 10: FEA torque function, mesh, and magnetic flux density with core magnet.

The function obtained was compared to the expected sinusoid function and exposes the actuator two equilibrium positions, one of which ($180°$), is unstable (see Fig. 10).

Each Samarium-Cobalt magnet is wrapped in a handcrafted two layer solenoid made of AWG30 wire ($N \approx 32$). The solenoids then are wired one after the other in a serial manner. The typical electrical characteristics of the solenoids and of the Halbach arrays as measured at $1kHz$ by a LCR meter (BK precision 878B) are:

$$\begin{cases} L_s \approx 7.2\mu H \\ R_s \approx 0.29\Omega \end{cases} \quad \begin{cases} L_H \approx 88\mu H \\ R_H \approx 3.5\Omega \end{cases} \tag{6}$$

The electrical circuit of the PPM is composed of a bank of 44 capacitors (42 ceramic StackiCap 2220-1K20224-X-WS2, $0.22\mu F$ each ; two film capacitor MKP1847, $3\mu F$ each, total measured capacitance: $15.4\mu F$). The capacitors discharge in each Halbach Array through a solid state switch (thyristor). For manufacturing simplicity, each of the Halbach array coils are wired independently and soldered onto intermediary printed circuit boards (PCBs) placed in the stator. Both these PCBs are then wired to a larger PCB holding the motor, capacitors, and thyristors, and designed to integrate into a Robotiq gripper. The actuator, the capacitor bank, and the thyristors are placed on a printed circuit board (PCB) designed to integrate fully into a Robotiq gripper.

The capacitors charge and thyristor activation are operated by an external PCB, controlled by a computer through the RS-232 communication protocol. This PCB is wired to an external high-voltage, high-current power supply (Iseg, HPp 20 407) and regulates both the capacitors' voltage and polarity. The full system's operation is illustrated in Fig. 11.

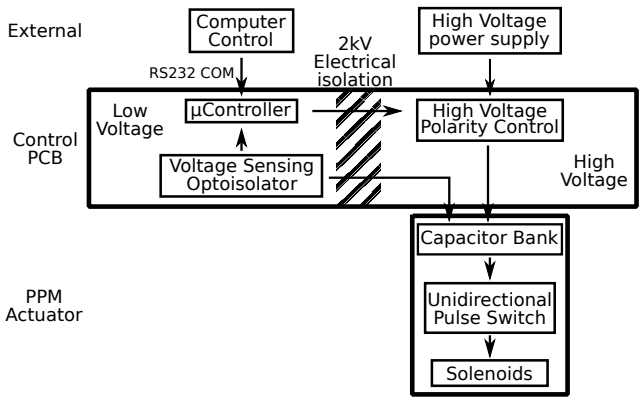

Figure 11: General System Diagram.

Figure 12: Robotiq 2-finger gripper with PPM actuator grabbing a stress ball.

The actuator's stator is divided into two parts that have been 3-D printed (Zortrax M200). The coils and magnets are then fixed inside and the assembly is fixed using flat bearings and non-conductive screws. The complete actuator with capacitors weighs about 200 grams.

The prototype was successfully integrated in a commercially available two finger Robotiq hand. When used in the under-actuated robotic hand, our prototype generated enough torque to open and close the gripper, allowing it to grasp various objects as demonstrated in Fig. 12.

Regarding the control the actuator: since the Halbach arrays are superposed with a shifted angle of $90°$, and since they are magnetized separately, for each magnetization the shaft can rotate by a maximum of $90°$. By using two stacked Halbach arrays and controlling the order in which they are magnetized, we control both the direction of the rotation and the amount of torque generated by the actuator. The amount of torque may be controlled separately because when the Halbach arrays' magnetic flux densities are changed, as long as the ratio of one Halbach array's magnetic flux density relative to the other remains unchanged, then the shaft position will be unchanged too, but the torque will be different.

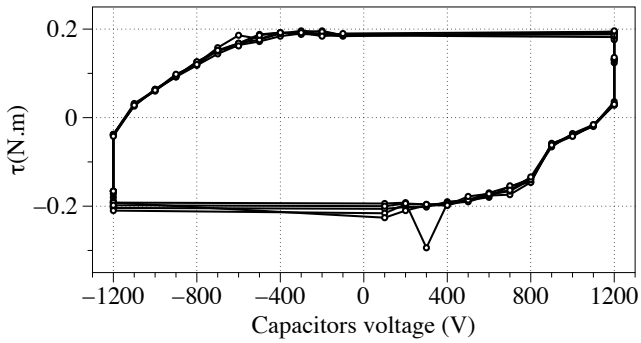

Figure 13: Experimental Actuator torque as a function of capacitors terminal voltage.

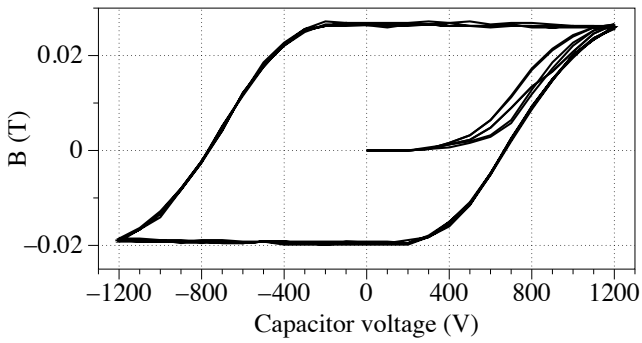

Figure 14: Experimental measure of the magnetic flux density at the center of one Halbach array.

V. Experimental Results

A. Actuator Torque Output

Fig. 13 represents the PPM actuator torque output as a function of the capacitors terminal voltage before discharging. Each data point is a mean between five torque acquisition, as measured 10 cm from the shaft rotation center by a force gauge (Mark 10, M4-10). The maximum torque is about 0.2 N.m. From Fig. 13, we can also observe that based on the capacitors' voltage, many different levels of torque output can be produced. Hence, torque is not simply an on/off function.

The torque theoretical (Fig 10) and experimental (Fig 13) maximum values are in good agreement (0.22 N.m and 0.2 N.m), slight disparities probably being due to unaccounted ferromagnetic material in the simulation (bearings, shaft), and imperfections in the magnets. Thanks to these results, we believe the shape of both numerically computed and experimental torque functions to correspond closely. This function is of great importance when using the actuator to generate passive torque.

B. Halbach Magnetic Flux Density

Experimental results of the magnetic field density generated by the Halbach array are shown in Fig. 14. As the capacitors pulses magnetize the Halbach array, the magnetic flux density is directly related to the capacitors voltage before discharge. The magnetic flux density was measured at the center of one of the two Halbach arrays using a Hall effect sensor (SS495A, Honeywell).

The pulse sequence was run 5 times, and logged autonomously by the microcontroller, as illustrated in Fig. 14. The voltages used for the pulses span from 1.2 kV to 100 V with a 100 V interval, and using 10 pulses at each voltage level. Although the curve resembles the shape of a magnetization curve, such as presented earlier in Fig. 5, it actually expresses the magnetic flux density (B) of the Halbach array as no applied magnetic field (H) was present. The measured magnetic flux density is also fairly low because the use of discrete magnets generates a non-uniform magnetic field that is weakest at the Halbach center.

C. Pulse Characterization

To magnetize any ferromagnetic material, one must generate large magnetic fields. However, these magnetic fields only have to be maintained during short periods of time (in the order of nanoseconds) for the magnets magnetic domains to align. In our case, the ferromagnetic material to be magnetized is the SmCo magnets that constitute the two Halbach arrays of the stator. All the magnets constituting one array are magnetized simultaneously and to the same level. Each Halbach array is magnetized separately.

As evidenced by the Hysteresis curves shown before in Fig. 5, the applied magnetic field needed to magnetize a magnet depends both on the magnet's coercivity and its previous magnetic state. High magnetic fields are required when the stator is strongly magnetized in the opposite direction, or if the ferromagnetic is very hard to magnetize.

We experimentally found that for the shaft to make a full rotation using the minimal amount of current pulses (4 pulses), the capacitors' voltage has to be at least 1150V. Fig. 15 shows experimental measure of 4 current pulses in one Halbach array, using capacitors at different voltages. The pulses were captured with an oscilloscope (Tektronix TDS 1002B) and through a rogowsky current waveform transducer (Powertek CWT 6B, 5 mV/A sensitivity).

Based on the current generated by the pulses (i), and using the number of wire turns in the solenoid (N), and the solenoid length (l) and diameter (d), we can estimate the applied

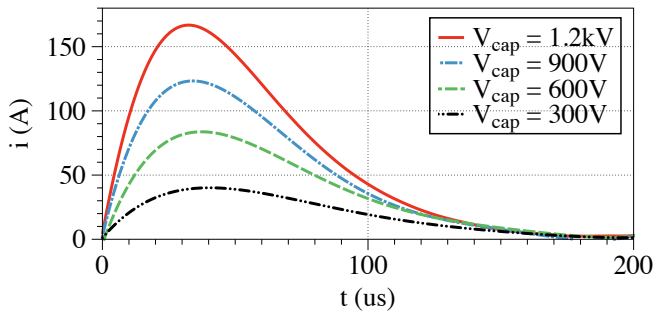

Figure 15: Current pulses in a single Halbach Array, depending on capacitors terminal charge voltage.

magnetic field (H) at the magnet's center in a solenoid of equal length and diameter ($d \approx l$),

$$H = \frac{Ni}{l}\left[\frac{l}{\sqrt{l^2+d^2}}\right] \approx \frac{Ni}{l\sqrt{2}} \tag{7}$$

Since multiple layers of wires are used in our solenoids, the Eq.7 only serves as an approximation. Using Eq. 7, a 1.2 kV charge of the capacitors, creating a 168 A current pulse, generates an applied magnetic field of approximately $598\ kA/m$, which is consistent with our magnet characteristics.

The energy contained in the capacitors is given by the Eq. 8. The energy contained in a capacitor depends on its voltage and capacitance. Since the capacitance is constant, it is the capacitor's voltage that dictates the energy of a pulse. Based on Eq. 8, the energy contained in the most powerful pulse is obtained by charging the capacitors at 1200 V, and contains approximately 11.1 Joules.

$$E_p = \frac{1}{2}CV^2 \tag{8}$$

In order to minimize weight and volume, a measure of capacitors energy density seems reasonable. The ceramic capacitors are capable of storing approximately ten times more energy per unit of volume than the Vishay film capacitors, and are easier to fit inside a given space. However, other factors such as safety, over voltage resistance, and peak current capability, are important too. In all these factors, the film capacitors are superior to the ceramic capacitors.

VI. Conclusion

In this paper we presented a completely new type of actuator named the programmable permanent magnet actuator. Contrary to classical electromagnetic motors that use constant current to generate magnetic fields, our actuator uses high transient current pulses to store magnetic fields in hard ferromagnetic material. By selecting a specific grade of ferromagnetic material we were able to create a stator that would not demagnetize when exposed to a strong neodymium magnetic field and be able to store a large magnetic field. Using a specific magnetic circuit called the Halbach Array, we focused the magnetic field in the stator, thus reducing magnetic flux leakage while also increasing the magnetic field strength.

The result of this work is an actuator which energetic characteristics are the opposite to other common types of actuators. This actuator passively generates torque and is particularly suited for low speed direct drive applications. We foresee pertinent use in fields such as robotic grasping, active prosthetics, and robotic legged locomotion. As an example, the PPM actuator prototype was integrated in a Robotiq two fingers hand and used to grasp various objects.

This groundbreaking work also leads to multiple avenues for optimization and improvements that will allow the actuator to gain in efficiency in the near future:

- Improved electrical circuit for improved resiliency and control of current pulse generation.
- Optimized electrical circuit depending on coils inductance and capacitors total capacitance.
- Improved actuator mechanical design and further optimization of the magnetic field.
- Creation of an hybrid actuator coupling the PPM actuator with a conventional electromagnetic motor. This may yield interesting results for improved motor bandwidth and rotational speed.
- Improved actuator control.

References

[1] Dura magnetics website. http://www.duramag.com/. Accessed: 2017-01-16.

[2] Nicadrone website ; opengrab epm. http://nicadrone.com/. Accessed: 2016-12-05.

[3] Wikipedia website ; electropermanent magnets. https://en.wikipedia.org/wiki/Electropermanent_magnet. Accessed: 2016-12-05.

[4] Julien Boisclair, Pierre-Luc Richard, Thierry Laliberte, and Clement Gosselin. Gravity compensation of robotic manipulators using cylindrical halbach arrays. *IEEE/ASME Transactions on Mechatronics*.

[5] Kyle Gilpin, Ara Knaian, and Daniela Rus. Robot pebbles: One centimeter modules for programmable matter through self-disassembly. In *Robotics and Automation (ICRA), 2010 IEEE International Conference on*, pages 2485–2492. IEEE, 2010.

[6] Klaus Halbach. Design of permanent multipole magnets with oriented rare earth cobalt material. *Nuclear instruments and methods*, 169(1):1–10, 1980.

[7] Ulrich Hochberg, Armin Dietsche, and Klaus Dorer. Evaporative cooling of actuators for humanoid robots. In *Proceedings of the 8th Workshop on Humanoid Soccer Robots, IEEE-RAS International Conference on Humanoid Robots, Atlanta*, 2013.

[8] Ara Nerses Knaian. *Electropermanent magnetic connectors and actuators: devices and their application in programmable matter*. PhD thesis, Citeseer, 2010.

[9] Toyotaka Kozuki, Hirose Toshinori, Takuma Shirai, Shinske Nakashima, Yuki Asano, Yohei Kakiuchi, Kei Okada, and Masayuki Inaba. Skeletal structure with artificial perspiration for cooling by latent heat for musculoskeletal humanoid kengoro. In *Intelligent Robots and Systems (IROS), 2016 IEEE/RSJ International Conference on*, pages 2135–2140. IEEE, 2016.

[10] Marc-Antoine Lacasse, Genevieve Lachance, Julien Boisclair, Jérémie Ouellet, and Clément Gosselin. On the design of a statically balanced serial robot using remote counterweights. In *Robotics and Automation (ICRA), 2013 IEEE International Conference on*, pages 4189–4194. IEEE, 2013.

[11] J Mallinson. One-sided fluxes–a magnetic curiosity? *IEEE Transactions on magnetics*, 9(4):678–682, 1973.

[12] Andrew D Marchese, Cagdas D Onal, and Daniela Rus. Soft robot actuators using energy-efficient valves controlled by electropermanent magnets. In *2011 IEEE/RSJ International Conference on Intelligent Robots and Systems*, pages 756–761. IEEE, 2011.

[13] Nicholas Paine, Joshua S Mehling, James Holley, Nicolaus A Radford, Gwendolyn Johnson, Chien-Liang Fok, and Luis Sentis. Actuator control for the nasa-jsc valkyrie humanoid robot: A decoupled dynamics approach for torque control of series elastic robots. *Journal of Field Robotics*, 32(3):378–396, 2015.

[14] Sangok Seok, Albert Wang, Meng Yee Chuah, David Otten, Jeffrey Lang, and Sangbae Kim. Design principles for highly efficient quadrupeds and implementation on the mit cheetah robot. In *Robotics and Automation (ICRA), 2013 IEEE International Conference on*, pages 3307–3312. IEEE, 2013.

[15] Junichi Urata, Toshinori Hirose, Yuta Namiki, Yuto Nakanishi, Ikuo Mizuuchi, and Masayuki Inaba. Thermal control of electrical motors for high-power humanoid robots. In *2008 IEEE/RSJ International Conference on Intelligent Robots and Systems*, pages 2047–2052. IEEE, 2008.

[16] Junichi Urata, Yuto Nakanishi, Kei Okada, and Masayuki Inaba. Design of high torque and high speed leg module for high power humanoid. In *Intelligent Robots and Systems (IROS), 2010 IEEE/RSJ International Conference on*, pages 4497–4502. IEEE, 2010.

[17] Patrick M Wensing, Albert Wang, Sangok Seok, David Otten, Jeffrey Lang, and Sangbae Kim. Proprioceptive actuator design in the mit cheetah: Impact mitigation and high-bandwidth physical interaction for dynamic legged robots. *IEEE Transactions on Robotics*, 2017.